applied sciences

MDPI

Article

New Bioadsorbent Derived from Winemaking Waste Cluster Stalks: Application to the Removal of Toxic Cr(VI) from Liquid Effluents

Lorena Alcaraz, Francisco J. Alguacil * and Félix A. López

National Center for Metallurgical Research (CENIM), Spanish National Research Council (CSIC), Avda. Gregorio del Amo 8, 28040 Madrid, Spain; alcaraz@cenim.csic.es (L.A.); f.lopez@csic.es (F.A.L.)

* Correspondence: fjalgua@cenim.csic.es

Received: 29 October 2020; Accepted: 15 December 2020; Published: 17 December 2020

Abstract: A winemaking waste was used as a precursor of activated carbon used for the removal of hazardous Cr(VI) from solutions. The preparation process consisted of a hydrothermal process and a chemical activation of the resulting product, with KOH. The adsorption results show that the adsorption of Cr(VI) on the obtained activated carbon is strongly dependent on the stirring speed applied to the carbon/solution mixture, pH of the solution, and temperature. The equilibrium isotherm was well fitted to the Langmuir Type-II equation, whereas the kinetic can be described by the pseudo-second-order kinetic model. Thermodynamic studies revealed that Cr(VI) adsorption was an exothermic and spontaneous process. Finally, desorption experiments showed that Cr(VI) was effectively desorbed using hydrazine sulfate solutions, and, at the same time, the element was reduced to the less hazardous Cr(III) oxidation state.

Keywords: activated carbon; winemaking waste; wastewater; Cr(VI) removal; adsorption process; Cr(VI) reduction

1. Introduction

It is known that water is a critical resource with wide uses, such as for urban, agricultural, and industrial purposes [1], and is a basic requirement for humans and wildlife. Unfortunately, this resource is finite, with no adequate substitute. Only a small amount of the water of the world is economically accessible for the previously cited purposes. The great increase in the world population leads to several forms of water pollution, as well as an increase in the global water demand [2]. Nowadays, industrial and urban activities have increased, causing subsequently water pollution, for example with heavy metals. These metals could be introduced by both natural sources (e.g., weathering of soils and rocks or from volcanic eruptions) and from anthropogenic activities (mining, processing, or use of metals). The most common heavy metal pollutants in water are Cd, Cr, Cu, Ni, Pb, and Hg.

The use of chromium in several applications such as electroplating, tanning, pigment manufacture, or biocides, among others, leads to great discharges of chromium-containing effluents into the environment [3]. The toxicity of the elements depends on its chemical form [4]. Chromium ions are present in environmental water principally in two different oxidation states: Cr(III) and Cr(VI). While Cr(III) is less soluble, has low toxicity, and is a required nutrient [3,5], Cr(VI) is toxic and carcinogenic. The continuous exposure of Cr(VI) causes important health problems such as epigastric pain, nausea and vomiting, diarrhea, hemorrhage, and even cancer in the digestive tract and lungs [6]. In addition, accordingly to the literature [7], Cr(VI) modifies the DNA transcription process, causing important chromosomic aberration. Even though chromium is usually present at low concentrations in environmental water, removal of this metal is an important topic.

Several techniques for chromium removal from wastewaters have been reported, including chemical precipitation [8], electrochemical precipitation [9], solvent extraction [10], ion exchange [11], and adsorption process [5,12,13]. Due to its simplicity, effectiveness, and low cost, the adsorption process has been extensively investigated for metal removal from aqueous solutions. However, the great inconvenience in the application of this process by industries is the cost of adsorbents. Generally, the cost of commercial adsorbent is very high, which is a barrier to using the adsorption process [6].

Activated carbons are useful adsorbent materials for the removal of a large variety of pollutants. It has been reported that it is possible to obtain them from renewable sources, such as from agro-industrial wastes and by new synthesis processes [14]. Among the great variety of wastes, winemaking waste is an attractive option due to the number of grapes produced worldwide and the amount of waste generated for winemaking [15]. Thus, the use of winemaking waste to obtain activated carbon and its use for heavy metals adsorption is an important aim in the scientific community for both heavy metal removal from wastewater and the reuse and recycling of a generated waste.

In this paper, an activated carbon (AC) derived from a waste generated in wine production, cluster stalks, is described. Cr(VI) removal by adsorption process was assessed. Different parameters that affect the adsorption process such as stirring speed, solution pH, temperature, ionic strength, and adsorbent dosage were evaluated. Adsorption isotherms and kinetic studies were also investigated. Finally, Cr(VI) recovery from Cr(VI)-loaded carbon was addressed in several experimental conditions.

2. Materials and Methods

2.1. Synthesis of the Activated Carbon

Activated carbon (AC) was obtained from a winemaking waste, cluster stalks, according to a previously described procedure [15]. For the sample preparation, an aqueous suspension of 75 g/L of cluster stalks (production of Albariño wine; Denomination of Origin "RíasBaixas", Galicia, Spain) was introduced into a high-pressure reactor at 30 bars and 250 °C for 3 h. After that, the final mixture was filtered obtaining a hydrothermal carbon as a precursor. To obtain the corresponding activated carbon, a mixture of precursor/KOH (1:2) was introduced in a tubular oven under a N_2 flow at 800 °C for 2 h. Finally, the obtained black solid was washed until a neutral pH was reached. More information about the characterization of the activated carbon can be found in [15].

2.2. Adsorption Experiments

Cr(VI) adsorption by the obtained activated carbon was performed via batch experiments, using a 250-mL glass reactor provided, mechanical shaking, and a 2.3-cm diameter four-blade glass impeller. The metal concentration of the solution was analyzed by flame atomic absorption spectrometry (AAS) using a Perkin Elmer 1100B spectrophotometer. The adsorption percentages were calculated by Equation (1):

$$\text{Adsorption}(\%) = \frac{[\text{Cr}]_{\text{aq},0} - [\text{Cr}]_{\text{aq},t}}{[\text{Cr}]_{\text{aq},0}} \text{x}100 \quad (1)$$

where $[\text{Cr}]_{\text{aq},0}$ and $[\text{Cr}]_{\text{aq},t}$ (mg/L) are the initial concentration and concentration at time t of Cr(VI) in the solution, respectively. The associated analytical error was within ±2%.

Different experiments were carried out to analyze several parameters which affect the adsorption process. Stirring speed was modified in the range 250–1500 min^{-1} in 200 mL of Cr(VI) solution (10 mg/L concentration), at pH 4, with 10 mg of the activated carbon. The solution pH was adjusted by adding suitable HCl and NaOH solutions until the desirable pH value was achieved using buffer solutions in calibrating pH meter. The temperature of the experiments was modified (in 10 °C incrememnts) between 20 and 60 °C. The temperature was controlled using a Selecta Termotronic thermostat-controlled bath. The effect of the ionic strength was investigated by adding different amounts of lithium chloride to the solutions of Cr(VI) of concentration 10 mg/L and 1 mg of the activated carbon. Finally, the adsorption equilibrium isotherms were analyzed varying the activated carbon amount between 0.5

and 100 mg using the Type-I Langmuir [16,17] (Equation (2)), Type-II Langmuir [18,19] (Equation (3)), Freundlich [20,21] (Equation (4)), and Temkin [22,23] (Equation (5)) linear forms using Origin Pro v.2019 software:

$$\frac{[Cr]_{aq,e}}{[Cr]_{c,e}} = \frac{1}{[Cr]_{c,m}K_L} + \frac{1}{[Cr]_{c,m}}x[Cr]_{aq,e} \quad (2)$$

$$\frac{1}{[Cr]_{c,e}} = \frac{1}{[Cr]_{c,m}} + \frac{1}{K_L[Cr]_{c,m}}x\frac{1}{[Cr]_{aq,e}} \quad (3)$$

$$\ln[Cr]_{c,e} = \ln K_F + \frac{1}{n}\ln[Cr]_{aq,e} \quad (4)$$

$$[Cr]_{c,e} = \frac{RT}{b_T}\ln A_T + \frac{RT}{b_T}\ln[Cr]_{aq,e} \quad (5)$$

where $[Cr]_{aq,e}$ (mg/L) is the concentration of the metal in solution at equilibrium, $[Cr]_{c,e}$ (mg/g) is the adsorbed metal amount per gram of activated carbon at equilibrium, $[Cr]_{c,m}$ is the maximum adsorbed metal amount per gram of activated carbon, K_L (L/mg) and K_F (L/g) are the corresponding Langmuir and Freundlich constants, 1/n (non-dimensional) is the adsorption intensity, A_T (L/g) is the Temkin isotherm equilibrium binding constant, and b_T (non-dimensional) is the Temkin isotherm constant.

The kinetic study was carried out using the pseudo-first- [24] and pseudo-second-order [25] kinetic models:

$$\ln\left([Cr]_{c,e} - [Cr]_{c,t}\right) = \ln[Cr]_{c,e} - k_1 t \quad (6)$$

$$\frac{t}{[Cr]_{c,t}} = \frac{1}{k_2[Cr]_{c,e}^2} + \frac{1}{[Cr]_{c,e}}t \quad (7)$$

In addition, the rate law which governs the adsorption process onto the adsorbent was analyzed by three possible adsorption mechanisms: film diffusion (Equation (8)) [26], particle diffusion (Equation (9)) [27], and moving boundary (Equation (10)) [22]:

$$\ln(1 - F) = -kt \quad (8)$$

$$\ln\left(1 - F^2\right) = -kt \quad (9)$$

$$3 - 3(1 - F)^{\frac{2}{3}} - 2F = kt \quad (10)$$

where k is the corresponding constant and F is the factorial approach to equilibrium (Equation (11)):

$$F = \frac{[Cr]_{c,t}}{[Cr]_{c,e}} \quad (11)$$

where $[Cr]_{c,t}$ and $[Cr]_{c,e}$ are the concentrations of metal loaded onto the carbon after an elapsed time and at equilibrium, respectively.

Finally, the thermodynamic parameters (standard enthalpy (ΔH^0), entropy (ΔS^0), and Gibbs free energy (ΔG^0)) were calculated using Equations (12)–(14) [28,29]:

$$\Delta G^0 = -RT\ln k_d \quad (12)$$

$$\ln k_d = \frac{\Delta S^0}{R} - \frac{\Delta H^0}{RT} \quad (13)$$

where k_d is the distribution coefficient (Equation (14)):

$$k_d = \frac{[Cr]_{c,e}}{[Cr]_{aq,e}} \quad (14)$$

2.3. Desorption Experiments

These experiments were also performed in glass reactors provided with glass impellers, as described above. To carry out these desorption experiments, 0.1 g of the Cr(VI)-loaded activated carbon was added to hydrazine sulfate solutions with a concentration of 10 g/L at 20 °C for 4 h. Different volumes of eluent solution were investigated for a fixed carbon amount. Cr(VI) desorption percentage and chromium concentration in the final solution were assessed.

3. Results and Discussion

3.1. Cr(VI) Adsorption Experiments

3.1.1. Stirring Speed

The stirring speed applied to the carbon solution may have a key role in the adsorption process due to modifying the mass gradient of adsorbate from the solution to the adsorbent interface [30]. Thus, different experiments were carried out to study the influence of this variable on the Cr(VI) adsorption process. An activated carbon dosage of 0.5 g·L^{-1} was added into Cr(VI) solutions of 0.01 g·L^{-1} (resulting pH 4) at 20 °C. Figure 1 exhibits the adsorption percentage of Cr(VI) after a contact time of 5 h versus the stirring speed. It can be observed that the adsorption process was influenced by stirring speed. Cr(VI) adsorption percentage increased with the stirring speed from 250 to 1500 min^{-1}. However, using higher stirring speeds decreased the adsorption percentage. Thus, these results indicate that the thickness of the aqueous boundary layer at 1000 min^{-1} was lowest and leads to a higher adsorption percentage. The decrease in the adsorption of Cr(VI) at higher stirring speeds could be due to the formation of local equilibria, which hinders the adsorption process [31,32]. According to these results, a stirring speed of 1000 min^{-1} was used in the subsequent experiments.

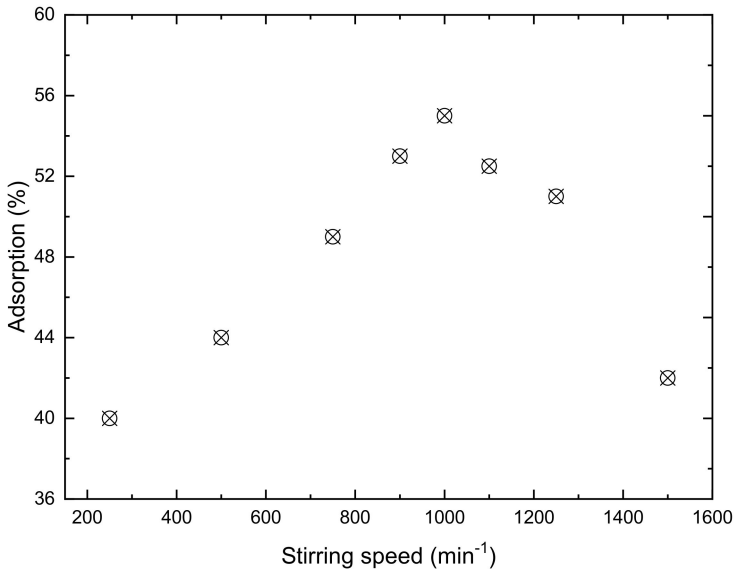

Figure 1. Influence of the stirring speed on the Cr(VI) adsorption.

3.1.2. pH of the Solution

As in the case of the stirring speed, the pH of the solution could play a significant role in the adsorption process of heavy metals [33] because this variable influences the surface charge of the adsorbent, the degree of ionization, and the species that the adsorbate forms in the corresponding solution [34]. In the case of Cr(VI), as shown in Figure 2, the pH value influenced the element speciation. In this figure, it can be observed that, at the concentration of 0.01 g/L Cr(VI), the same concentration

used in the present investigation, the metals are present as $HCrO_4^-$ and CrO_4^{2-} species, at pH values of 0–6 and 8–14, respectively.

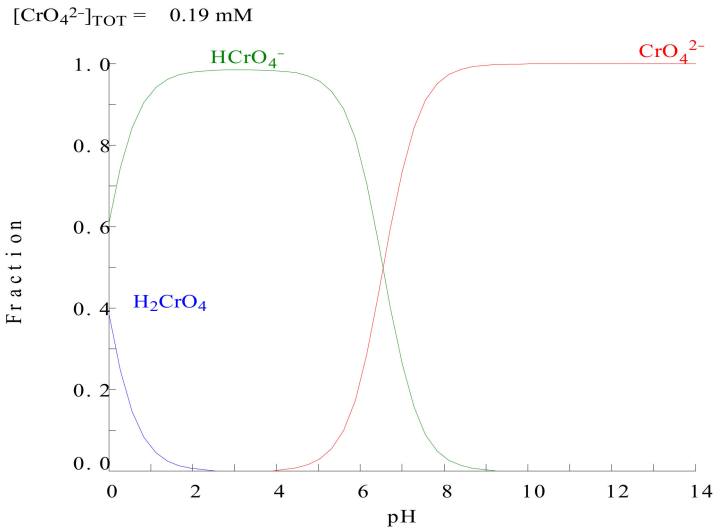

Figure 2. Cr(VI) speciation as pH function [35].

Thus, metal uptake onto the carbon was investigated as a function of this variable, and the results of these series of tests are represented in Figure 3. These results indicate that the adsorption percentage dramatically increased from pH 0 to 3, with the maximum Cr(VI) adsorption percentage (90%) being at pH 3. Thereafter, metal uptake decreased until a constant percentage of 38% resulted at pH values higher than 8. These results are due to the carbon surface becoming positively charged at acid pH values [36,37]; thus, when the solution pH increases, the surface losses its positive charge. These results are in good agreement with those previously reported [36], where the obtained value of the isoelectric point for the investigated activated carbon was 1.42.

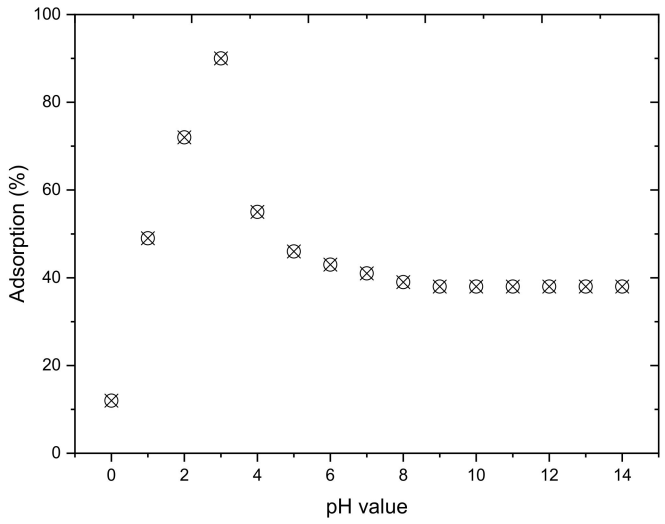

Figure 3. Cr(VI) adsorption percentage as a function of the solution pH. Aqueous phase: 0.01 g/L Cr(VI) at different pH values. Carbon dosage: 0.5 g/L. Temperature: 20 °C. Time: 5 h. Stirring speed: 1000 min^{-1}.

Accordingly, at pH ≥ 8, Cr(VI) adsorption became constant, the reason probably being due to one (or a combination) of three effects: (i) decrease of the positive charge of the AC; (ii) less adsorption

capacity of the carbon to adsorb CrO_4^{2-} species; or (iii) a competition of CrO_4^{2-} and OH^- species to be adsorbed onto the carbon. Based on the above, a pH of 3 was used in the subsequent experiments.

3.1.3. Effect of the Temperature

The temperature at which the process is carried out could improve or hamper the adsorption process. The adsorption percentage as a function of the different temperatures used is shown in Figure 4. As can be seen, an increase of the temperature resulted in a drastic decrease of Cr(VI) removal from the solution. The adsorption efficiency decreased with the temperature due to the probable decrease in ion mobility and its tendency to be adsorbed onto the activated carbon surface, as well as the increase of temperature decreasing the activity of the binding sites on the adsorbent surface [38]. Thus, the calculated adsorption percentages varied between 45% (at 20 °C) and 3% (at 60 °C). These results reveal that an increase of the temperature hampered the Cr(VI) adsorption process from the solution onto the activated carbon.

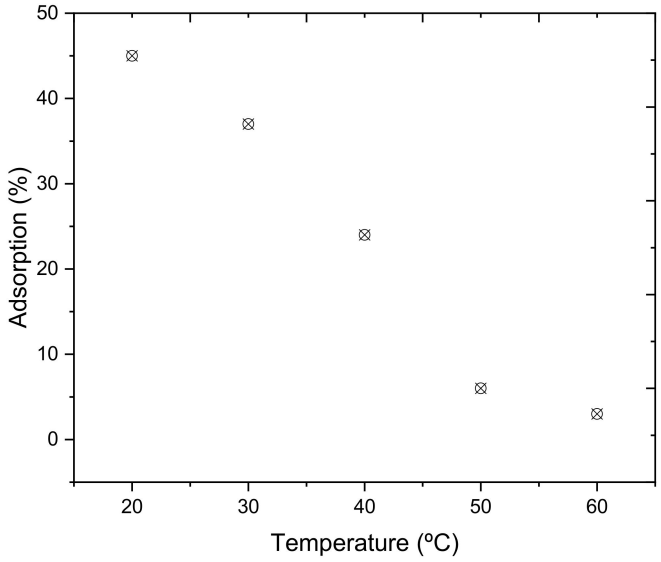

Figure 4. Cr(VI) adsorption at different temperatures. Aqueous phase: 0.01 g/L Cr(VI) at pH 3. Carbon dosage: 0.5 g/L. Time: 5 h. Stirring speed: 1000 min^{-1}.

3.1.4. Effect of the Ionic Strength

There are usually other metallic and nonmetallic components in addition to the metal to be removed present in the liquid solution. These components could affect its ionic strength, thus the effect of this parameter on the adsorption process is also interesting to investigate. Figure 5 exhibits that, when the ionic strength increased, it dramatically reduced the adsorption percentage, being the same tendency shown with other adsorbents [39]. The obtained results reveal that the electrostatic forces between the activated carbon surface and Cr(VI) ions were attractive [40].

3.1.5. Influence of the Adsorbent Dosage

The effect of the adsorbent dosage on the Cr(VI) adsorption process was also evaluated. Figure 6 shows the obtained results from the different experiments carried out. As expected, metal removal increased with the increase of the adsorbent dosage and for a fixed metal concentration because the number of binding sites available for ions adsorption increased [38]. It should be noted that, for an extremely low adsorbent dose (i.e., $2.5 \cdot 10^{-3}$ g/L), an adsorption percentage exceeding 30% was found. In addition, for 0.5 g/L adsorbent, the Cr(VI) adsorption was almost quantitative.

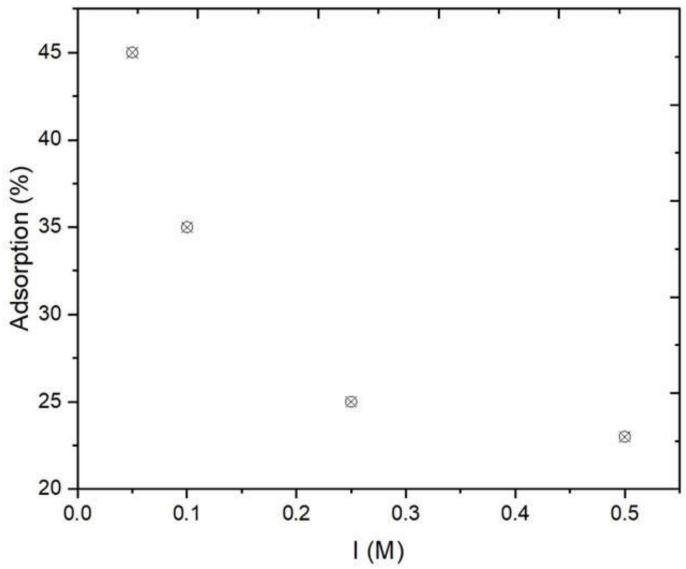

Figure 5. Effect of solution ionic strength on the Cr(VI) adsorption process. Aqueous phase: 0.01 g/L Cr(VI) at pH 3. Carbon dosage: 0.5 g/L. Temperature: 20 °C. Time: 5 h. Stirring speed: 1000 min^{-1}.

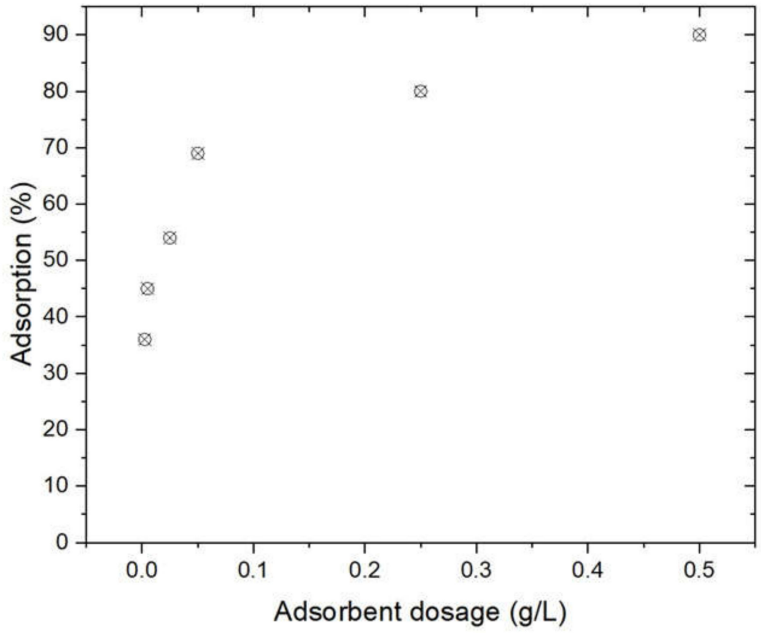

Figure 6. Effect of the adsorbent dosage on the Cr(VI) adsorption process. Aqueous phase: 0.01 g/L Cr(VI) at pH 3. Temperature: 20 °C Time: 5 h. Stirring speed: 1000 min^{-1}.

3.2. Adsorption Isotherms, Kinetic Study and Rate Law

To analyze the adsorption isotherm associated with the metal uptake onto the adsorbent, the results presented in Section 3.1.5 were fitted to various adsorption isotherms using Equations (2)–(5). The results of these fits, as shown in Figure 7, indicate that the highest correlation coefficient (R^2 = 0.9667) was obtained for the Langmuir isotherm Type-II, being K_L estimated as 0.01 L/mg. Moreover, R_L is defined as:

$$R_L = \frac{1}{1 + K_L[Cr]_{aq,0}} \quad (15)$$

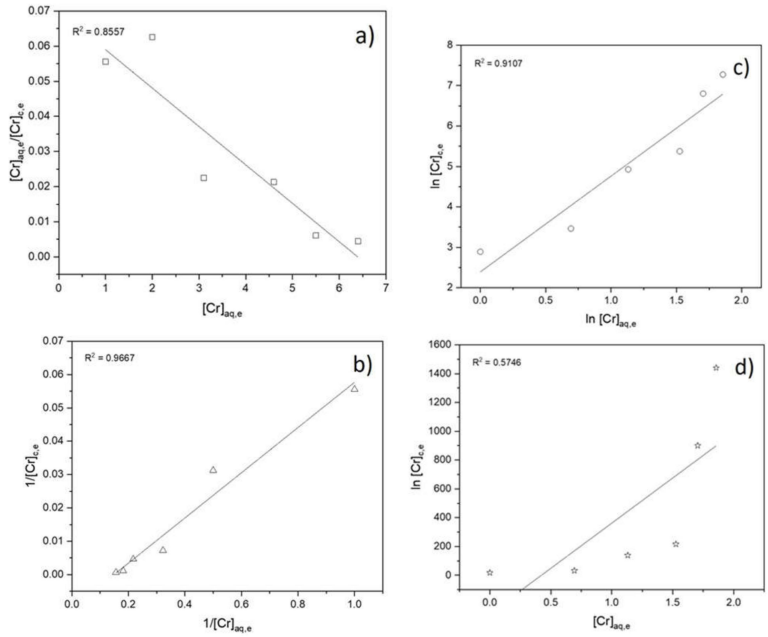

Figure 7. Linearized Type-I Langmuir (**a**); Type-II Langmuir (**b**); Freundlich (**c**); and Temkin (**d**) adsorption isotherms.

It was found that the process is favorable since $R_L < 1$.

Adsorption kinetics provides information about the uptake rate of adsorbate onto the adsorbent and controls the residual time during the adsorption process [41]. To analyze the mechanism controlling the kinetic adsorption process, the obtained data were fitted using Equations (6) and (7), and the adjustments are shown in Figure 8. The results from the fit indicate that the best correlation coefficient ($R^2 = 0.9976$) was obtained for the pseudo-second-order kinetic model, estimating a calculated kinetic constant of 0.0014 L/mg·min.

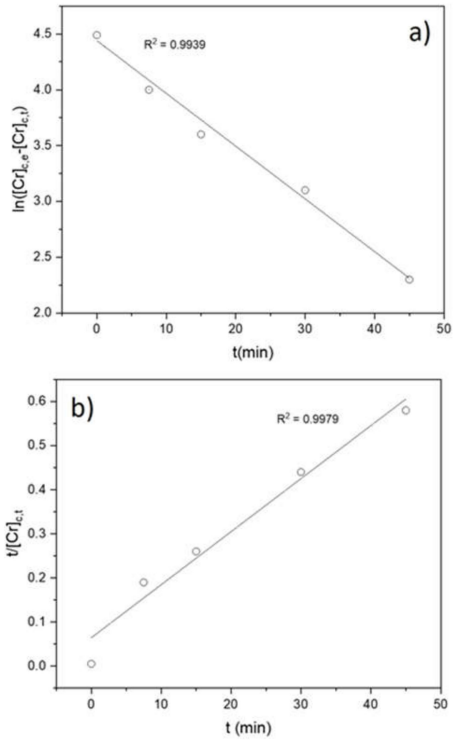

Figure 8. Pseudo-first-order (**a**); and pseudo-second-order (**b**) kinetics models for Cr(VI) adsorption.

To determine the probable rate law governing the Cr(VI) adsorption, the experimental data were fitted to Equations (8)–(10), as shown in Figure 9. The best fit (R^2 = 0.9969) was found within the film-diffusion model, with a calculated rate constant of 0.0473 min^{-1}.

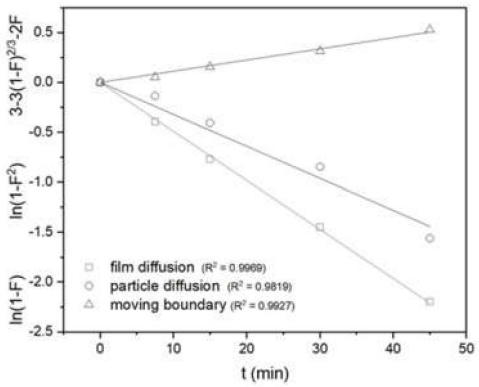

Figure 9. Linear adjustments of the rate law.

Finally, from the results presented in Section 3.1.3, the thermodynamic parameters were calculated using Equations (14) and (15). The negative value obtained for the standard enthalpy (−71 kJ/mol) was indicative of the exothermic nature of the adsorption process. The negative calculated value for the entropy (−13 J/mol·K) indicated a decrease of the randomness in the Cr(VI) uptake onto the carbon. Despite this, in all cases, the calculated Gibbs free energy change was negative, revealing that the adsorption is a spontaneous process.

3.3. Desorption Process

Table 1 summarizes the results derived from the different desorption experiments. It is shown that an increase in the volume of the eluent solution did not influence the percentage of Cr(VI) desorption, reaching values of around 50%; however, the chromium concentration in the resulted solution increased as the volume of solution/carbon weight relationship decreased. The reduction of Cr(VI) to Cr(III) responded to the next reaction:

$$4HCrO_4^- + 10H^+ + 3N_2H_4{\cdot}H_2SO_4 \rightarrow 4Cr^{3+} + 16H_2O + 3N_2 + 3SO_4^{2-} \quad (16)$$

Table 1. Desorption results.

Volume of the Solution/Carbon Weight	[Cr(III)]aq,t (mg/L)	Desorption (%)
2000	4	49
1000	9	50
500	17	49
250	34	50

In the present case, Cr(VI) was reduced to Cr(III), which is described as having low toxicity [3,5]. In addition, as a result of the low solubility of the Cr(III), it can be precipitated, leading to Cr_2O_3 and/or $Cr(OH)_3$, which could be used as a pigment [42–44].

4. Conclusions

Activated carbon (AC) from winemaking waste was obtained by a hydrothermal process, followed by a chemical activation of the resultant product with KOH. In the experimental procedure, an aqueous suspension of cluster stalks was treated at 30 bars and 250 °C for 3 h in a high-pressure reactor. After that, the obtained hydrothermal solid was activated with KOH at 800 °C for 2 h. The final

AC was used for Cr(VI) removal from aqueous solution. Several parameters were investigated. The maximum adsorption percentage was found at 1000 min^{-1} and a solution pH of 3. An increase in the adsorbent dosage improved the percentage of the Cr(VI) adsorption process. The effect of the temperature on the process revealed that an increase of the temperature led to a decrease in the chromium removal. Thus, the adsorption is an exothermic process, with a calculated standard enthalpy of −71 kJ/mol, being the process spontaneous in nature. In addition, the negative obtained entropy value (−13 J/mol·K) indicated the decrease of the randomness in the final system. Cr(VI) uptake onto the activated carbon responded well to the Langmuir Type-II isotherm model as well as the pseudo-second-order kinetic model. The rate law associated with the adsorption process resulted to be governed by a film-diffusion process. Cr(VI) can be desorbed by the use of hydrazine sulfate solutions. The desorption process rendered chromium as less toxic and potentially profitable, as a pigment product, Cr(III) oxidation state in the solution.

Author Contributions: F.J.A. and F.A.L. conceived the study. L.A. and F.J.A. carried out the experiments. L.A. and F.J.A. wrote the manuscript. All authors contributed to the review, editing, and approval of the paper. All authors have read and agreed to the published version of the manuscript.

Funding: This research received no external funding.

Acknowledgments: The authors thank the Viticulture Group at the Misión Biológica de Galicia (CSIC) for providing the winemaking waste used in the present work.

Conflicts of Interest: The authors declare no conflict of interest.

References

1. Yang, H.; Ye, S.; Zeng, Z.; Zeng, G.; Tan, X.; Xiao, R.; Wang, J.; Song, B.; Du, L.; Qin, M.; et al. Utilization of biochar for resource recovery from water: A review. *Chem. Eng. J.* **2020**, *397*, 125502. [CrossRef]
2. Joseph, L.; Jun, B.M.; Flora, J.R.V.; Park, C.M.; Yoon, Y. Removal of heavy metals from water sources in the developing world using low-cost materials: A review. *Chemosphere* **2019**, *229*, 142–159. [CrossRef]
3. Brdar, M.; Šćiban, M.; Takači, A.; Došenović, T. Comparison of two and three parameters adsorption isotherm for Cr(VI) onto Kraft lignin. *Chem. Eng. J.* **2012**, *183*, 108–111. [CrossRef]
4. Kot, A. The role of speciation in analytical chemistry. *TrAC Trends Anal. Chem.* **2000**, *19*, 69–79. [CrossRef]
5. Dai, J.; Ren, F.L.; Tao, C. Adsorption of Cr(VI) and speciation of Cr(VI) and Cr(III) in aqueous solutions using chemically modified chitosan. *Int. J. Environ. Res. Public Health* **2012**, *9*, 1757–1770. [CrossRef]
6. Cronje, K.J.; Chetty, K.; Carsky, M.; Sahu, J.N.; Meikap, B.C. Optimization of chromium(VI) sorption potential using developed activated carbon from sugarcane bagasse with chemical activation by zinc chloride. *Desalination* **2011**, *275*, 276–284. [CrossRef]
7. U.S. Department of Health and Human Services. Toxicological Profile for Chromium. *ATSDR Toxicol. Profiles*. 2012. Available online: www.atsdr.cdc.gov/toxprofiles (accessed on 17 December 2020).
8. Audin, F.; Soylak, M. A novel multi-element coprecipitation technique for separation and enrichment of metal ions in environmental samples. *Talanta* **2007**, *73*, 134–141. [CrossRef]
9. Kongsricharoern, N.; Polprasert, C. Chromium removal by a bipolar electro-chemical precipitation process. *Water Sci. Technol.* **1996**, *34*, 109–116. [CrossRef]
10. Yasuaki, O.; Yoshitaka, N.; Hiderou, N.; Kazuyuki, I.; Terufumi, F.K.T. High preconcentration of ultra-trace metal ions by liquid–liquid extraction using water/oil/water emulsions as liquid surfactant membranes. *Microchem. J.* **2000**, *65*, 341–346.
11. Tiravanti, G.; Petruzzelli, D.; Passino, R. Pretreatment of tannery wastewaters by an ion exchange process for Cr(III) removal and recovery. *Water Sci. Technol.* **1997**, *36*, 197–207. [CrossRef]
12. Alguacil, F.J.; López, F.A. Removal of Cr(VI) from Waters by Multi-Walled Carbon Nanotubes: Optimization and Kinetic Investigations. In *Water and Wastewater Treatment*; IntechOpen: London, UK, 2019.
13. Dönmez, G.; Aksu, Z. Removal of chromium(VI) from saline wastewaters by Dunaliella species. *Process Biochem.* **2002**, *38*, 751–762. [CrossRef]
14. Beltrame, K.K.; Cazetta, A.L.; de Souza, P.S.C.; Spessato, L.; Silva, T.L.; Almeida, V.C. Adsorption of caffeine on mesoporous activated carbon fibers prepared from pineapple plant leaves. *Ecotoxicol. Environ. Saf.* **2018**, *147*, 64–71. [CrossRef]

15. Alcaraz, L.; López Fernández, A.; García-Díaz, I.; López, F.A. Preparation and characterization of activated carbons from winemaking wastes and their adsorption of methylene blue. *Adsorpt. Sci. Technol.* **2018**, *36*, 1331–1351. [CrossRef]
16. Alguacil, F.J.; Escudero, E. Removal of arsenic(V) from aqueous wastes by ion exchange with Lewatit MP64 resin. *Desalin. WATER Treat.* **2018**, *133*, 257–261. [CrossRef]
17. Al-Ghamdi, Y.O.; Alamry, K.A.; Hussein, M.A.; Marwani, H.M.; Asiri, A.M. Sulfone-modified chitosan as selective adsorbent for the extraction of toxic Hg(II) metal ions. *Adsorpt. Sci. Technol.* **2019**, *37*, 139–159. [CrossRef]
18. Abd El Salam, H.; Sharara, T. A novel microwave synthesis of manganese based MOF for adsorptive of Cd(II), Pb(II) and Hg(II) ions from aqua medium. *Egypt. J. Chem.* **2019**, *62*, 837–851. [CrossRef]
19. Alguacil, F.J. La eliminación de metales tóxicos presentes en efluentes líquidos mediante resinas de cambio iónico. Parte XIII: Zinc(II)/H+/Lewatit OC-1026. *Rev. Metal.* **2020**, *56*, 172. [CrossRef]
20. Wang, X.; Cui, S.; Yan, B.; Wang, L.; Chen, Y.; Zhang, J. Isothermal Adsorption Characteristics and Kinetics of Cr Ions onto Ettringite. *J. Wuhan Univ. Technol. Sci. Ed.* **2019**, *34*, 587–595. [CrossRef]
21. Elbadawy, H.A. Adsorption and structural study of the chelating resin, 1,8-(3,6-dithiaoctyl)-4-polyvinyl benzenesulphonate (dpvbs) performance towards aqueous Hg(II). *J. Mol. Liq.* **2019**, *277*, 584–593. [CrossRef]
22. Chanda, M.; Rempel, G.L. Quaternized Poly(4-vinylpyridine) Gel-Coated on Silica.Fast Kinetics of Diffusion-Controlled Sorption of Organic Sulfonates. *Ind. Eng. Chem. Res.* **1994**, *33*, 623–630. [CrossRef]
23. Nethaji, S.; Sivasamy, A. Adsorptive removal of an acid dye by lignocellulosic waste biomass activated carbon: Equilibrium and kinetic studies. *Chemosphere* **2011**, *82*, 1367–1372. [CrossRef]
24. Lagergren, S. Zur Theorie der sogenannten Adsorption gelöster Stoffe. *Zeitschrift für Chemie und Ind. der Kolloide* **1907**, *2*, 15.
25. Ho, Y.; McKay, G. Pseudo-second order model for sorption processes. *Process Biochem.* **1999**, *34*, 451–465. [CrossRef]
26. Chiarizia, R.; Horwitz, E.P.; Alexandratos, S.D. Uptake of metal ions by a new chelating ion-exchange resin. Part 4: Kinetics. *Solvent Extr. Ion Exch.* **1994**, *12*, 211–237. [CrossRef]
27. Saha, B.; Iglesias, M.; Dimming, I.W.; Streat, M. Sorption of tace heavy metals by thiol containing chelating resins. *Solvent Extr. Ion Exch.* **2000**, *18*, 133–167. [CrossRef]
28. Liu, W.; Jiang, X.; Chen, X. Synthesis and utilization of a novel carbon nanotubes supported nanocables for the adsorption of dyes from aqueous solutions. *J. Solid State Chem.* **2015**, *229*, 342–349. [CrossRef]
29. El-Aila, H.J.; Elsousy, K.M.; Hartany, K.A. Kinetics, equilibrium, and isotherm of the adsorption of cyanide by MDFSD. *Arab. J. Chem.* **2016**, *9*, S198–S203. [CrossRef]
30. Sanchez, N.; Benedetti, T.M.; Vazquez, M.; De Torresi, S.I.C.; Torresi, R.M. Kinetic and thermodynamic studies on the adsorption of reactive red 239 by carra sawdust treated with formaldehyde. *Adsorpt. Sci. Technol.* **2012**, *30*, 881–899. [CrossRef]
31. Alcaraz, L.; Alguacil, F.J.; López, F.A. Microporous adsorbent from winemaking waste for the recovery of Mn(VII) in liquid solutions. *Can. J. Chem. Eng.* **2020**. [CrossRef]
32. Alguacil, F.J.; Lopez, F.A.; Rodriguez, O.; Martinez-Ramirez, S.; Garcia-Diaz, I. Sorption of indium (III) onto carbon nanotubes. *Ecotoxicol. Environ. Saf.* **2016**, *130*, 81–86. [CrossRef]
33. Degefu, D.M.; Dawit, M. Chromium removal from modjo tannery wastewater using moringa stenopetala seed powder as an adsorbent topical collection on remediation of site contamination. *Water. Air. Soil Pollut.* **2013**, *224*, 1719. [CrossRef]
34. Yue, X.; Huang, J.; Jiang, F.; Lin, H.; Chen, Y. Synthesis and characterization of cellulose-based adsorbent for removal of anionic and cationic dyes. *J. Eng. Fiber. Fabr.* **2019**, *14*, 155892501982819. [CrossRef]
35. Puigdomenech, I. Medusa Program. Available online: www.kth.se/che/medusa (accessed on 17 December 2020).
36. Alguacil, F.J.; Alcaraz, L.; García-Díaz, I.; López, F.A. Metals Removal of Pb 2+ in Wastewater via Adsorption onto an Activated Carbon Produced from Winemaking Waste. *Metals* **2018**, *8*, 697. [CrossRef]
37. Alcaraz, L.; García-Díaz, I.; Alguacil, F.J.; Lopez, F.A. Removal of Copper Ions in Wastewater by Adsorption onto a Green Adsorbent from Winemaking Wastes. *BioResources* **2020**, *15*, 1112–1133.
38. Javadian, H.; Ruiz, M.; Saleh, T.A.; Sastre, A.M. Ca-alginate/carboxymethyl chitosan/$Ni_{0.2}Zn_{0.2}Fe_{2.6}O_4$ magnetic bionanocomposite: Synthesis, characterization and application for single adsorption of Nd+3, Tb+3, and Dy+3 rare earth elements from aqueous media. *J. Mol. Liq.* **2020**, *306*, 112760. [CrossRef]

39. Yin, R.; Niu, Y.; Zhang, B.; Chen, H.; Yang, Z.; Yang, L.; Cu, Y. Removal of Cr(III) from aqueous solution by silica-gel/PAMAM dendrimer hybrid materials. *Environ. Sci. Pollut. Res.* **2019**, *26*, 18098–18112. [CrossRef]
40. Al-Degs, Y.S.; El-Barghouthi, M.I.; El-Sheikh, A.H.; Walker, G.M. Effect of solution pH, ionic strength, and temperature on adsorption behavior of reactive dyes on activated carbon. *Dyes Pigments* **2008**, *77*, 16–23. [CrossRef]
41. Gao, J.; Qin, Y.; Zhou, T.; Cao, D.; Xu, P.; Hochstetter, D.; Wang, Y. Adsorption of methylene blue onto activated carbon produced from tea (*Camellia sinensis* L.) seed shells: Kinetics, equilibrium, and thermodynamics studies. *J. Zhejiang Univ. Sci. B* **2013**, *14*, 650–658. [CrossRef]
42. Alguacil, F.J. Facilitated Chromium(VI) Transport across an Ionic Liquid Membrane Impregnated with Cyphos IL102. *Molecules* **2019**, *24*, 2437. [CrossRef]
43. Liang, S.; Zhang, H.; Luo, M.; Luo, K.; Li, P.; Xu, H.; Zhang, Y. Colour performance investigation of a Cr_2O_3 green pigment prepared via the thermal decomposition of CrOOH. *Ceram. Int.* **2014**, *40*, 4367–4373. [CrossRef]
44. Sangeetha, S.; Basha, R.; Sreeram, K.J.; Narayanan, S.; Nair, B. Functional pigments from chromium(III) oxide nanoparticles. *Dyes Pigments* **2012**, *94*, 548–552. [CrossRef]